

Article

Visual Characteristics of Afterimage under Dark Surround Conditions

Hung-Chung Li ¹ and Pei-Li Sun ^{2,*}

¹ Department of Cosmetic Science, Chang Gung University of Science and Technology, Taoyuan 33303, Taiwan; hcli01@mail.cgust.edu.tw

² Graduate Institute of Color and Illumination Technology, National Taiwan University of Science and Technology, Taipei 10607, Taiwan

* Correspondence: plsun@mail.ntust.edu.tw

Abstract: Three psycho-visual experiments were carried out to investigate visual afterimage characteristics of high luminance LEDs under dark surround conditions. The results show that the luminance of illumination, exposure time and background luminance are the primary factors influencing the afterimage's duration, the color difference between stimulus and background, and visibility. Besides, visual afterimage characteristics are strongly correlated with the luminance contrast between the stimulus and the background, but not for the color difference with a white background. A third-order polynomial regression model was proposed to accurately estimate the afterimage duration, the color difference between stimulus and background, and visibility. The model performance showed high R-squared, low root-mean-square error (RMSE) and mean absolute error (MAE) values between the predicted and visual characteristics.

Keywords: afterimage; viewing glare; illumination engineering; mesopic vision; regression analysis



Citation: Li, H.-C.; Sun, P.-L. Visual Characteristics of Afterimage under Dark Surround Conditions. *Energies* **2021**, *14*, 1404. <https://doi.org/10.3390/en14051404>

Academic Editor:
Alessandro Cannavale

Received: 4 February 2021
Accepted: 25 February 2021
Published: 4 March 2021

Publisher's Note: MDPI stays neutral with regard to jurisdictional claims in published maps and institutional affiliations.



Copyright: © 2021 by the authors. Licensee MDPI, Basel, Switzerland. This article is an open access article distributed under the terms and conditions of the Creative Commons Attribution (CC BY) license (<https://creativecommons.org/licenses/by/4.0/>).

1. Introduction

With the rapid development of solid-state lighting technology, white LED light efficiency has gradually increased in recent years. LED lighting technology can be seen widely in our daily life, such as in LED backlight modules, information boards and lighting applications. However, the LED dot matrix's high luminance characteristics might easily cause a dazzling glare, disturbing human vision and damaging the visual system, especially the retina [1,2]. As the driver looks directly toward the high luminance LED brake light from the front vehicle under night driving conditions, it causes an intense green afterimage on the retina, influencing road safety [3,4]. Humans initially perceive glare when subjected to a very bright light source, and this is replaced with an afterimage which subsequently appears [5,6]. The visual afterimage is considered as "flash blindness" which occurs with the temporary bleaching of photoreceptors on the retina.

1.1. Glare

Glare can be divided into two classes, discomfort and disability glare, respectively. The significant difference is that the latter can strongly obstruct visual performance. Previous studies have investigated the impact of glare induced by LED technology—Ixtaina et al. simulated night-time driving conditions to explore the perturbation or discomfort of glare. The LED signals that were directly visible and with refractors were compared. The findings showed that the higher punctual luminance raised the observers' perturbation and discomfort [7]. Tyukhova et al. implemented a glare rating experiment to determine how glare source luminance, source positions, source sizes and background luminance influenced pupil size and discomfort glare perception. Their results suggested that an increase of glare source luminance induced more discomfort in the observer [8]. Moreover, the visual data were evaluated with four discomfort glare models. The highest correlation with the

observer's response was achieved by a Unified Glare Rating (UGR) small source extension, and the model was further improved for dark surrounds and night-time applications [9]. Two experiments were carried out by Bullough et al. to test the discomfort from traffic signals, simulated with two distances and three signal colors. The results showed that higher discomfort presented with the increase of signal luminance and a decrease in the viewing distance. Regarding the color signal aspect, the green and yellow signals can easily cause visual discomfort [10]. How the age affected glare recovery, which is the recovery of contrast discrimination after exposure to a high luminance, was discussed by Collins et al. The recovery time was prolonged over 56 years of age [11]. Chen et al. examined the discomfort glare of light sources with different correlated color temperatures (CCTs) from 3100 to 5300 K. The modified UGR model, which took CCT into account, predicted glare perception more accurately and showed a high correlation of determination values [12]. Moreover, Sun et al. developed an image-based measurement system to evaluate the UGR value of fixation points from given panoramic scene images [13].

1.2. Visual Afterimage

Gazing at the high luminance stimulus might bring about a visual afterimage. Depending on the duration time, there were two types of visual afterimage presented, as shown in Figure 1. As the stimulus was removed, a brief positive afterimage was displayed which then gradually changed to a negative one in a relatively slow process [14]. For the positive afterimage, the light and dark parts corresponded to those of the object, whereas complementary colors appeared in the negative one [15]. In general, with a longer fixation duration, a significant negative afterimage is perceived. However, the afterimage's intense influence was determined by the positive one and was slightly colored [16]. Due to the disadvantages of afterimage on visual performance, many studies have contributed to investigating afterimage characteristics which result from a high luminance stimulus [17,18]. Reidenbach et al. adopted special eye test tasks such as the Landolt C visual test, or a reading task, to investigate the effects of exposure duration on the afterimage and visual impairment using colored LEDs. The results indicated that even exposure durations of less than a second would lead to significant vision impairment [19]. They also studied the characteristics of temporary blinding from various light sources, including LEDs and lasers. The visual acuity and the size of an afterimage as a function of duration caused by a high luminance white LED were quantified and modeled by linear and exponential regression. The experiment revealed that the afterimage size diminished after about 12 min, and the visual acuity was recovered between 30 and 60 s [20]. The visual acuity could be formulated as a logarithmic function depending on the duration of impairment [21]. Stimulus with a lower power laser resulted in a relatively longer duration time of afterimage which might interfere with visual performance up to 300 s [22]. Additionally, two lasers with wavelengths of 632.8 and 542 nm and red, green, blue, and white LEDs with high brightness, were used as the stimuli to establish the relationship between their afterimages and the visual acuity recovery time under low ambient lighting conditions [23]. Comparing the visual acuity recovery times of different light sources indicated that temporary blinding from LEDs impaired the color vision, and the blue LED affected it the most. On the other hand, the visual acuity was severely reduced by the green and white LEDs [24]. Regarding the afterimage's color appearance, Reidenbach et al. reported the color variation corresponded to the time sequence. The study summarized that the decrease in optical energy was related to the displacement of the perceived colors and would shorten the color variation process [25]. Mikamo et al. proposed a model to describe the color transitions in afterimages based on psychophysical experiments [26]. Furthermore, color discrimination and contrast sensitivity were tested from colored LEDs after displaying a dazzling glare. The result found that a decrease in one level of contrast would extend the identification time by about 4 s [27].

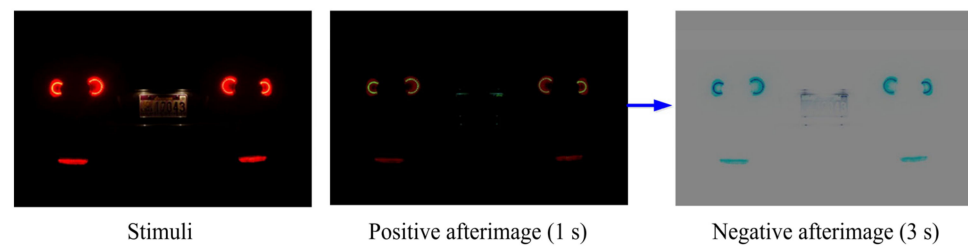


Figure 1. The transformation of afterimage.

From a review of the previous work, the afterimage's persistence was found to depend on the luminance of the light source, duration of exposure, surrounding luminance and the location of the effect [28]. Regarding road lighting design for night-time driving tasks, Brémond et al. suggested an index called the visibility level that is highly correlated with the detection distances [29]. The research revealed that accounting for the impact of visual afterimage characteristics is essential for advanced lighting studies. Determining how to account for the effects of visual afterimage characteristics is an initial step in the study of advanced lighting.

To cope with various LED lighting issues, the International Commission on Illumination (CIE) recently focused on researching the mesopic range of lighting characteristics, especially for night conditions [30,31]. The study aims to investigate the characteristics of visual afterimage caused by high luminance LEDs, including three experiments: (1) duration time of afterimage, (2) color difference between afterimage and background, (3) the impacts of afterimage to text visibility. Different luminance levels of illumination, exposure time, color stimuli and luminance of backgrounds were tested to explore the relationship between afterimage characteristics and influential factors.

2. Methods

2.1. Experimental Setup

A total of 60 test patterns were assessed for each evaluation item (duration of the afterimage, color difference, and visibility) with two luminance levels of illumination, five colors, three luminance levels of background and two exposure times. Figure 2 illustrates an example of a viewing field seen in a completely dark environment. An RGB LED spotlight presents all the stimuli with an IR remote control, enabling the adjustment of colors, transitions, and luminance levels. A half-silvered mirror (50% reflection and 50% transmission) was placed 70 cm in front of the observers to simultaneously acquire the stimulus and different luminance of the background, presented by a 47-inch narrow-bezel transparent display (47TS50MF, LG) with a resolution of 1920×1080 pixels. The circular stimulus viewing angle was about 1.35° at the subject's position, and a cross mark was placed at the center of the half-mirror as a fixation point. Tables 1 and 2 show the parameter settings. Each LED's luminance was measured by a spectroradiometer (SR-UL1R, TOPCON) at the observer's viewing position, and the colorimetric characteristics of the five achromatic colors are listed in Table 3. The black, gray, and white background luminance was 0.02, 9.76, and 29.16 cd/m^2 , respectively. Figures 3 and 4 illustrate the CIE (International Commission on Illumination) 1976 u', v' chromaticity coordinates of the LED color stimuli and the detail of viewing conditions, respectively.



Figure 2. An example of the viewing field.

Table 1. Parameters of the afterimage experiment.

| Stimulus Color | Red | Green | Blue | Yellow | White |
|------------------------|-----------|------------|------|-------------|-------|
| Background (Grayscale) | Black (0) | Gray (128) | | White (255) | |
| Exposure Time | 1 s | | | 3 s | |

Table 2. Luminance (cd/m^2) of five colors (through a half-mirror).

| (cd/m^2) | Red | Green | Blue | Yellow | White |
|----------------------------|--------|--------|------|--------|--------|
| Level 1 | 4376 | 7101 | 1308 | 12,031 | 10,365 |
| Level 2 | 18,165 | 29,095 | 5163 | 47,416 | 40,579 |

Table 3. Colorimetric characteristics of the five achromatic colors.

| Color | (R, G, B) | (u' , v') | Uniformity |
|--------|-----------------|------------------|------------|
| Red | (255, 0, 0) | (0.5367, 0.5194) | 0.186 |
| Green | (0, 255, 0) | (0.0705, 0.5776) | 0.374 |
| Blue | (0, 0, 255) | (0.1685, 0.1344) | 0.294 |
| Yellow | (255, 255, 0) | (0.2657, 0.5532) | 0.299 |
| White | (255, 255, 255) | (0.2034, 0.4197) | 0.377 |

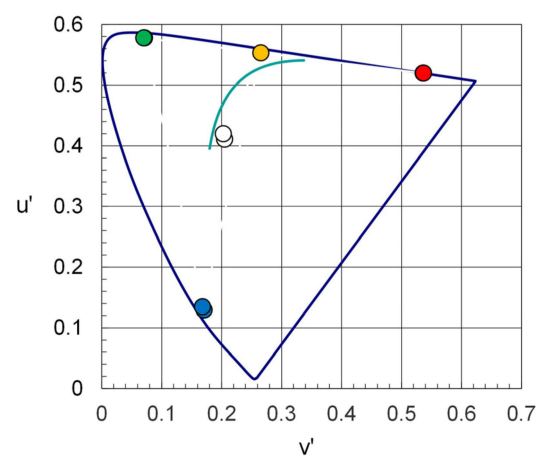


Figure 3. The CIE 1976 u' , v' chromaticity coordinates of the LED color stimuli.

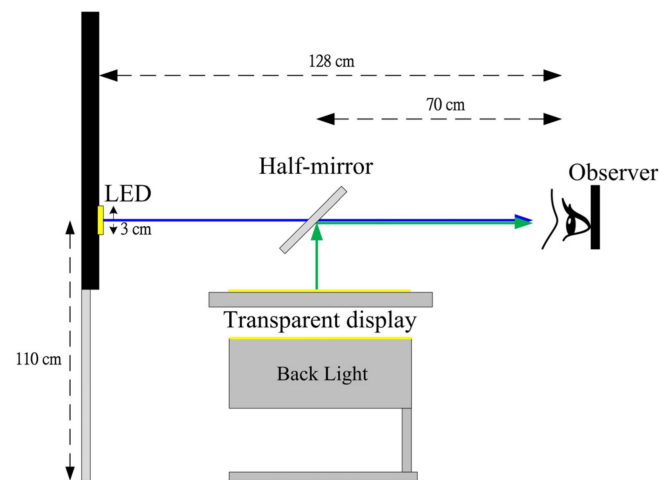


Figure 4. Illustration of the viewing conditions.

2.2. Experimental Procedures

Three psychophysical experiments were conducted to obtain visual data from observers. Before starting the experiments, a 20-min dark adaptation was required. During the experiment, each observer was seated in front of a half-silvered mirror in a completely dark environment. An experimenter sitting next to the blackout system controlled the display of stimuli in the same order and recorded the observer's assessments. The transition of the background and the control of exposure time were implemented with Matlab software. Twelve observers with normal vision, including seven males and five females, participated in each experiment. The observers were around 26 years of age (Mean = 25.83, SD = ± 1.99), and all of them were Taiwanese. Before starting the experiment, all observers had passed the Ishihara test for color deficiency. Each observer assessed two-fifths of the patterns twice for verification and adapted to the background for 10 s before the stimulus was presented.

2.2.1. Duration Time

For measuring the afterimage duration, a Graphical User Interface (GUI) was developed based on Matlab software to switch the background luminance and automatically calculate the duration, utilizing a timer to record the start and end times. The start time was the moment the high luminous stimulus was turned off. After the perceived negative afterimage disappeared, the observer was asked to click the mouse button as the end time. For better understanding the characteristics of the duration time, the positive afterimage from the green color stimulus was also studied.

2.2.2. Color Difference

In the grading of the color difference between the afterimage and background, a series of color difference grayscale images was displayed with the background on the half-mirror simultaneously after the stimulus was presented. Figure 5a shows examples of grayscale for different backgrounds. After 1 s and 5 s from stimulus removal, the observer had to judge the grayscale level and ascertain the relative color difference. The grayscale series from left to right were assigned as follows: level 0 to 8 for black, -4 to 4 for gray and -8 to 0 for a white background, respectively. The negative rating values signify the afterimage is relatively darker than the background. Moreover, levels 9, 5, and 1 were allowed for estimating an over bright afterimage in each background.



Figure 5. Illustration of (a) grayscale series in each background (b) low-contrast characters.

2.2.3. Visibility

The assessment of visibility was conducted by evaluating the rating scale to understand the impact of afterimage on visibility. The low-contrast characters shown in Figure 5b appeared in 3 s at the center of the half-mirror as the stimulus was removed. The observers needed to estimate the visibility with a rating level from 1 (unclear) to 8 (clear). Similar to the duration time task, two GUI applications were individually applied to the experiment for color difference and visibility and to simulate the background with grayscale and characters.

3. Results

3.1. Observer Variability

In previous studies, the coefficient of variation (CV) and correlation coefficient measure (r) were primarily adopted to investigate the agreement between two data sets. The data points can be plotted with a 45° line to reveal the circumstances of two sets of data in variation. The CV values were formulated as Equations (1) and (2) for estimating the inter-observer and intra-observer variability, respectively. The larger CV value means a poorer agreement.

$$CV = 100 \times \sqrt{\frac{1}{N} \sum \frac{(\Delta E - f \times \Delta V)^2}{(\Delta \bar{E})^2}}, f = \frac{\sum \Delta E \times \Delta V}{\sum (\Delta V)^2} \quad (1)$$

$$CV = \frac{100}{\bar{y}} \times \sqrt{\sum \frac{(x_i - y_i)^2}{N}} \quad (2)$$

where ΔV is the estimation of a stimulus from an individual observer, ΔE is the geometric mean of ΔV from all observers and $\Delta \bar{E}$ is the arithmetic mean of all evaluated stimuli N . The scaling factor f was used to adjust the data between ΔV and ΔE . Besides, the observer repeatability was calculated with Equation (2), where \bar{y} is the arithmetic mean of set y_i , and x_i and y_i represent the first and second judgments from the same observer.

Tables 4 and 5 show the mean results of the observer variability in each experiment. The observer variability in the color difference and visibility experiments were acceptable except for the duration. The reason is that the partly different retinal photoreceptors of the human eye may lead to higher observer variability. Therefore, the correlation coefficient measure (r) was applied to observer variability of the duration time, which showed better agreement. The r values were 0.86 and 0.85 for inter-observer and intra-observer variability, respectively. The photoconversion process of the afterimages was naturally different among the observers, such that the situation of the afterimages perceived at 5 s showed a significantly poorer agreement, excluding the white background, where the afterimage disappeared within a relatively shorter duration.

Table 4. Observer variability of duration and visibility.

| Characteristics | Inter (CV) | Intra (r) | Inter (r) |
|-----------------|------------|-----------|-----------|
| Duration Time | 35% | 0.85 | 0.86 |
| Visibility | 17% | 0.91 | 0.91 |

Table 5. Observer variability of color difference estimation.

| Background (CV) | Inter (CV) | | Intra (CV) | |
|-----------------|------------|-----|------------|-----|
| | 1 s | 5 s | 1 s | 5 s |
| Black | 15% | 34% | 10% | 22% |
| Gray | 10% | 19% | 6% | 11% |
| White | 15% | 9% | 8% | 6% |

3.2. Duration Time of Afterimage

The visual data were obtained by ignoring the data with a worse correlation coefficient of observer variability and averaging the rest of the observers' responses. Referring to Figure 6a,b, the results indicate that the afterimage duration increased with the higher contrast between the stimulus and backgrounds, where the black one required the longest time for elimination. Furthermore, the higher luminance of illumination and longer exposure time (Pattern 4) lead to a significantly more positive afterimage duration. The duration with different exposure times and luminance levels of the five color stimuli is shown in Figure 6c, where the ordinate represents the mean duration time of three backgrounds. As can be seen, the exposure time and luminance level were the primary factors that influenced the duration time. As the luminance level and exposure time increased, the duration time intensively increased and the luminance level (Level 2) showed a more significant impact on the duration compared with the exposure time (3 s). During the experiment period, a phenomenon was found in that the afterimage reappeared after the observers blinked, and the study from Ito [32] proposed a similar result. Additionally, the Pearson correlation coefficient between different backgrounds is listed in Table 6, presenting a similar tendency under three background levels.

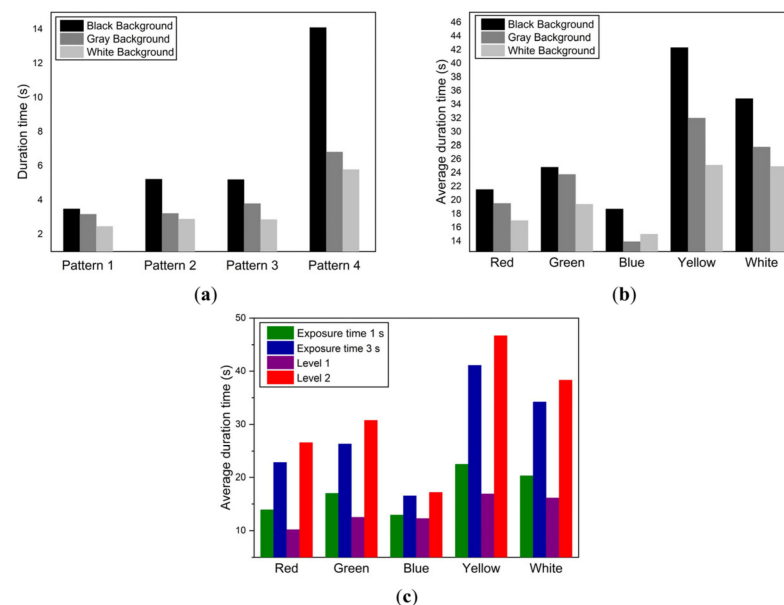
**Figure 6.** Duration of afterimage. (a) Positive afterimage in different backgrounds; (b) Duration in different backgrounds; (c) Duration with different exposure times and luminance levels.

Table 6. The correlation coefficient of the duration for each background.

| Characteristics | Black vs. Gray | Gray vs. White | White vs. Black |
|-----------------|----------------|----------------|-----------------|
| Duration Time | 0.97 | 0.95 | 0.95 |

3.3. Color Difference

In discussing the color difference between the afterimage and the background, all visual rating data were first converted to the absolute values. The mean color difference of the afterimage with different backgrounds was analyzed with acceptable visual data which had passed the observer variability exam, as shown in Figure 7a. According to the stacked bar chart, the brighter background, especially when presented with higher luminous stimuli, significantly reduced the color difference. Moreover, the higher luminous stimuli enlarged the color difference perceived by the observers for all background conditions. The impacts of luminance and exposure times were compared, as shown in Figure 7b, where the luminance level produced much more influence on the color difference at 1 s. Furthermore, Table 7 shows the correlation coefficient between different backgrounds on the color difference, and lower correlation was found when compared to the visual response of the white background. However, the black and gray backgrounds were highly correlated with each other.

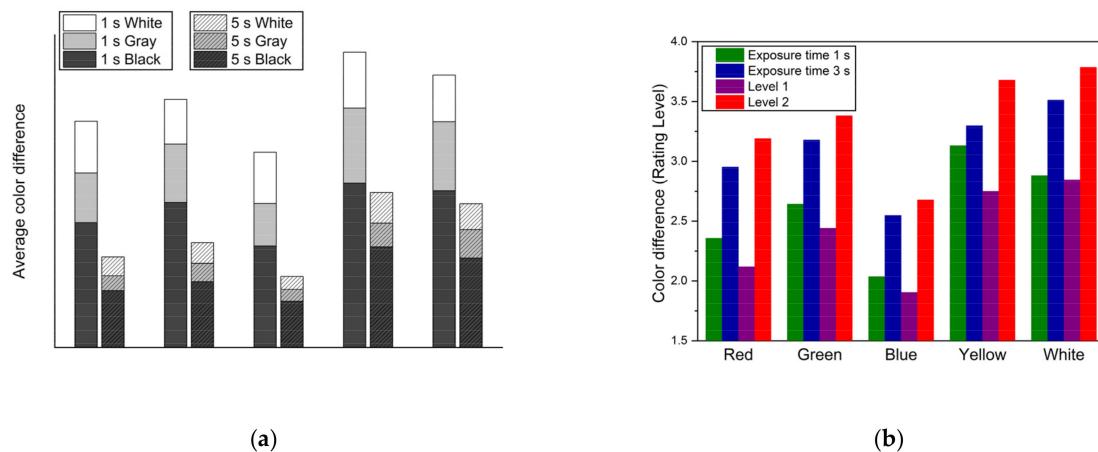


Figure 7. Color difference between the afterimage and background (a) with different background levels at 1 and 5 s; (b) with different exposure times and luminance levels.

Table 7. The correlation coefficient of the color difference between each background.

| Characteristics | Black vs. Gray | Gray vs. White | White vs. Black |
|------------------|----------------|----------------|-----------------|
| Color Difference | 0.97 | 0.67 | 0.57 |

3.4. Visibility

For visibility, the visual data were analyzed by ignoring the extreme data and averaging the observers' evaluations. Referring to Figure 8a, the visibility rating level was obviously influenced by backgrounds and decreased with the darker one. As shown in Figure 8b, visibility is significantly reduced with longer exposure time and higher luminance. Furthermore, the higher luminance level showed more potent effects. Throughout the experiment, it was suggested that the positive afterimage seriously obstructed vision. When discussing the correlation coefficient r between the different backgrounds regarding the visibility, high r values in Table 8 were presented by the comparison and similar to the duration.

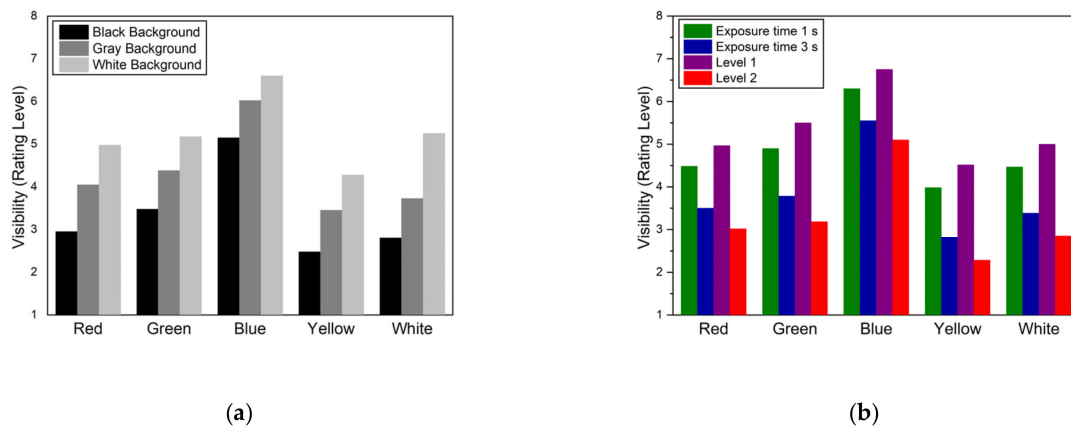


Figure 8. Afterimage visibility (a) in different backgrounds (b) with different exposure time and luminance level.

Table 8. The correlation coefficient of visibility between each background.

| Characteristics | Black vs. Gray | Gray vs. White | White vs. Black |
|-----------------|----------------|----------------|-----------------|
| Visibility | 0.99 | 0.97 | 0.96 |

3.5. Regression Analysis

For the regression analysis, linear regression and a polynomial regression model were utilized to describe the relationship between the visual characteristics of the afterimage resulting from high luminous LEDs under a completely dark environment. Due to there being just a smidgen of visual data for each background condition, only the linear regression was discussed to avoid overfit. However, the polynomial regression, which is typically used to fit the nonlinear dataset, was adopted to build the lighting application model.

The relationship between the duration and the experimental parameters which contained the luminance levels, the background luminance and the exposure time, was investigated. The integral of the luminance contrast of background with the exposure time was regarded as the linear regression feature. It was normalized initially with the highest luminance under each background level. The visual afterimage duration (DT) was formulated as Equation (3), where L_s and L_b are the luminance of the test stimulus and background in units of candela per square meter, and t_e represents the exposure time of the stimulus in seconds. a_0 and a_1 are the coefficients equivalent to the linear function intercept and slope, respectively, and their values are listed in Table 9 for different backgrounds. The result of the linear regression model showed highly positive correlations between the prediction and the visual response, where the r values are 0.96 for black, 0.99 for gray, and 0.94 for white backgrounds, as shown in Figure 9.

$$DT = a_1 \cdot \frac{L_s}{L_b} \cdot t_e + a_0 \quad (3)$$

Table 9. Optimal coefficients for fitting the duration.

| Coefficient | Black | Gray | White |
|-------------|-------|-------|-------|
| a_0 | 11.93 | 10.54 | 9.62 |
| a_1 | 66.91 | 52.08 | 27.74 |

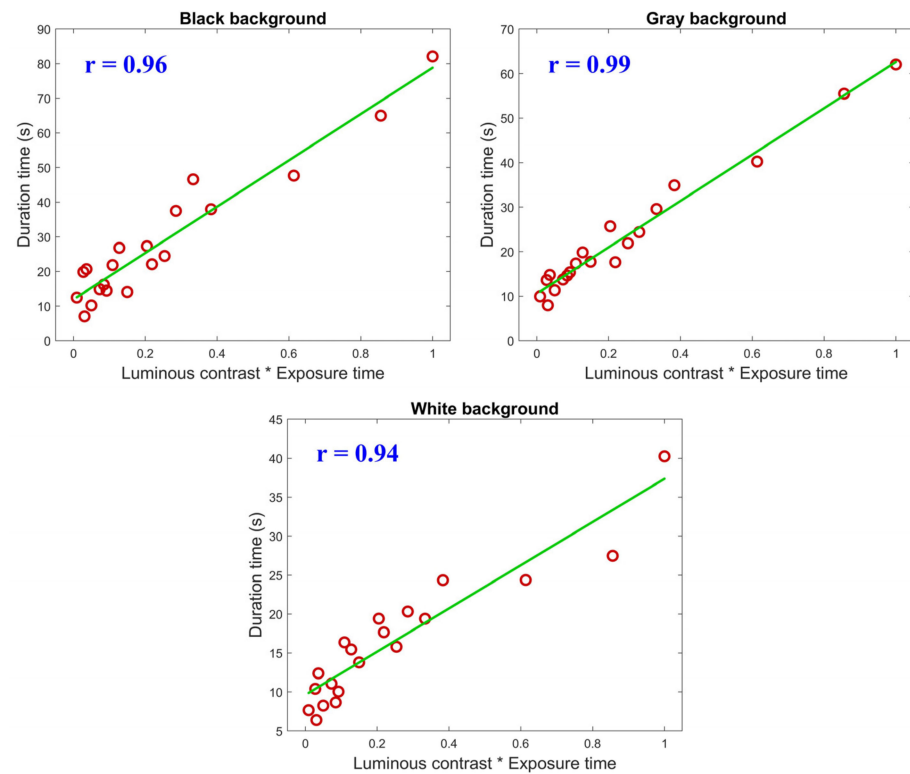


Figure 9. Relationship between the duration and luminance contrast with exposure time.

The color difference, denoted as CD, between the visual afterimage and background, can be modeled by the integral action from the logarithm of luminance contrast and exposure time as Equation (4). The optimal coefficients of linear regression are shown in Table 10. The r values are 0.96, 0.92 and 0.64 for black, gray and white backgrounds and the scatter plot of the prediction is illustrated in Figure 10. The result clearly showed that the correlations decrease with the raising of contrast, and the brightest background performs the poorest. This might be due to the conversion speed of the afterimage. From the above section of the duration time, the result illustrates the afterimage quickly disappears with the brighter background. Some observers immediately perceived a brighter positive afterimage as the higher luminous stimuli was removed in that process. A darker afterimage was then rapidly generated in 1 s, but some were still situated at the procedure of a positive afterimage. Although the perceived positive afterimage was brighter than the background at 1 s, the level of its color difference was no stronger than its highest level in the negative process. The difference in the personal conversion cycle was considered the main factor leading to a low correlation for a white background.

$$CD = b_1 \cdot \log\left(\frac{L_s}{L_b} \cdot t_e\right) + b_0 \quad (4)$$

Table 10. Optimal coefficients for fitting the color difference.

| Coefficient | Black | Gray | White |
|-------------|-------|-------|-------|
| b_0 | −8.46 | −2.43 | 0.37 |
| b_1 | 2.25 | 1.37 | 0.49 |

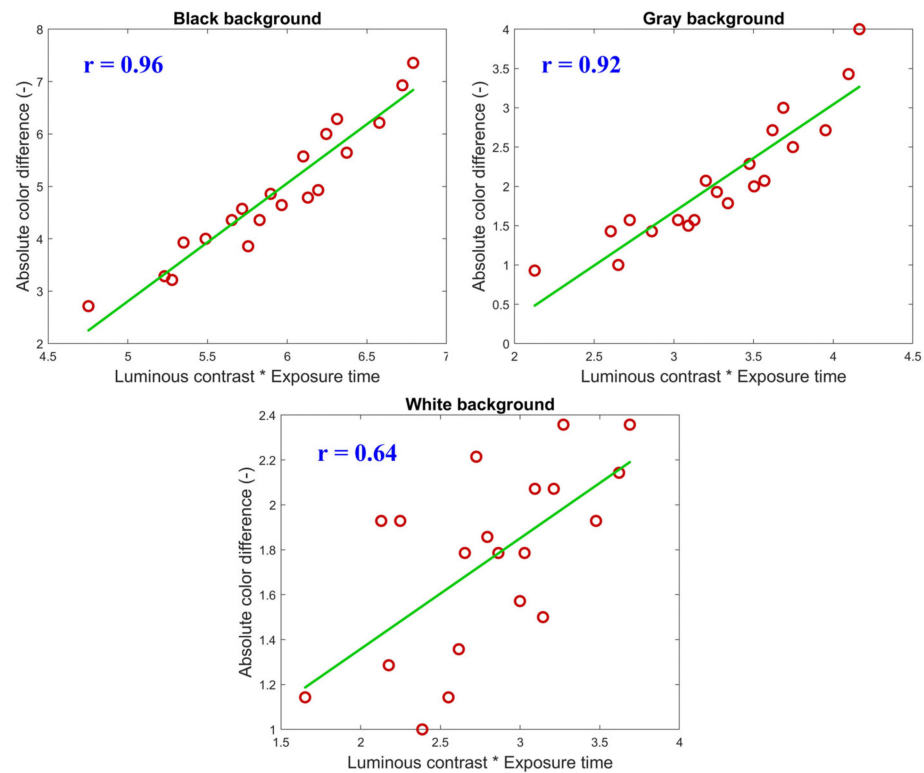


Figure 10. Relationship between absolute color difference and luminance contrast with exposure time (Stimulus/Background).

In terms of visibility (V), it can also be predicted indirectly by an identical linear function as that of color difference. In other words, the interference of visual performance is a negative presentation of visibility. The higher visibility implies a worse visual performance, which means that the observer cannot clearly recognize the characters. Hence, Equation (5) was used to quantify the degree of visual interference and reveal the opposite tendency with visibility. Following the Weber–Fechner law, the visibility depends on the logarithm of luminance contrast between stimulus and background. Table 11 lists the optimal coefficients of linear regression to predict the visibility. The high negative correlation presents with -0.95 , -0.96 , and -0.92 for black, gray, and white sets, as shown in Figure 11.

$$V = c_1 \cdot \log\left(\frac{L_s}{L_b} \cdot t_e\right) + c_0 \quad (5)$$

Table 11. Optimal coefficients for fitting the visibility.

| Coefficient | Black | Gray | White |
|-------------|---------|---------|---------|
| c_0 | 19.02 | 13.30 | 12.51 |
| c_1 | -2.65 | -2.73 | -2.58 |

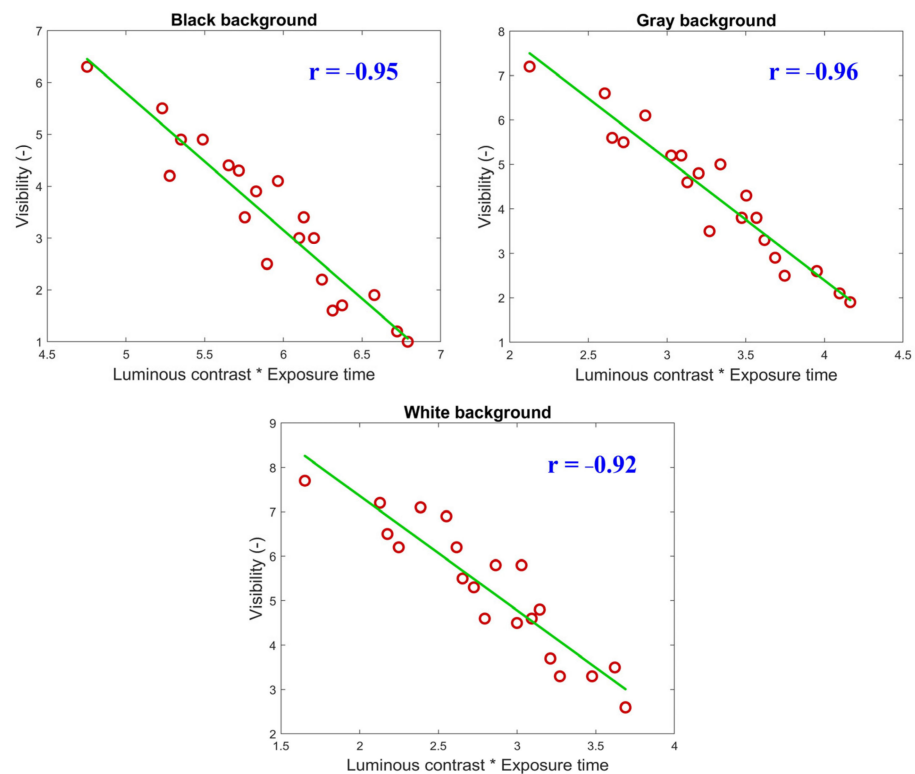


Figure 11. Relationship between visibility and luminance contrast with exposure time (Stimulus/Background).

4. Modeling

Following the outcome of the linear regression analysis, it was indicated that all of the afterimage visual characteristics were associated with the difference between the stimulus and background luminance except for the color difference under the white background. Like the functional expression of UGR estimation, the luminance contrast was the primary feature used to describe the visual performance of the afterimage.

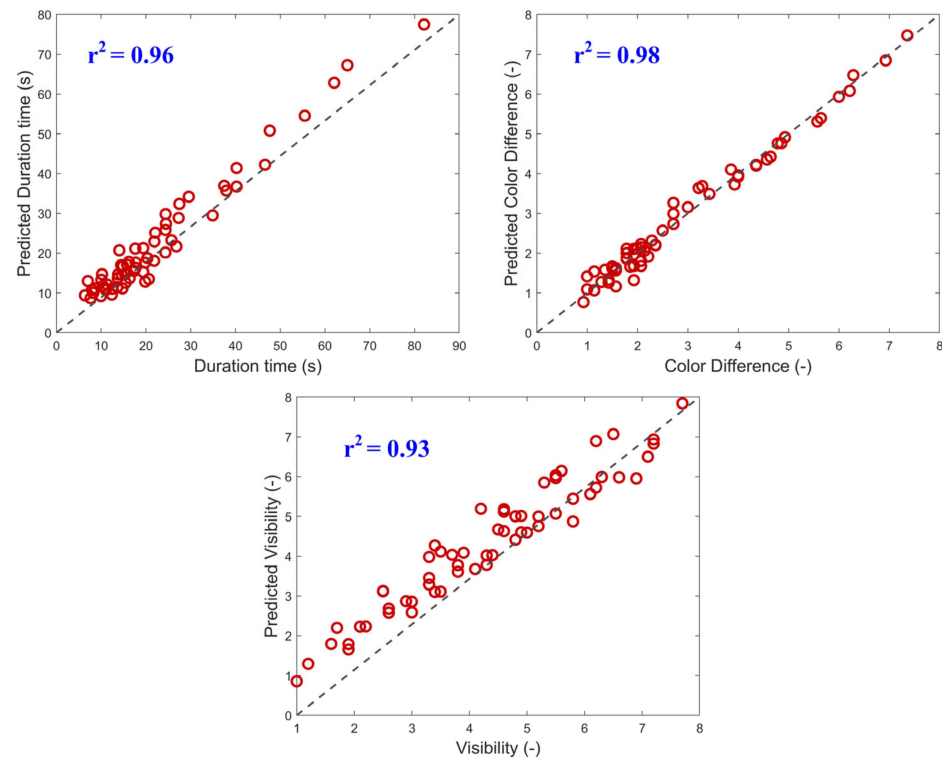
For developing a machine learning model, the luminance of the stimulus (L_s) and background (L_b), and the exposure time (t_e) were selected as the inputs for the training process. The afterimage visual characteristics, denoted as VC, were regarded as the output values including the duration time, color difference against the background and the visibility. They can be modeled by a third-order polynomial regression, as shown as Equation (6). The number of the parameters was 14 for the polynomials. The psycho-visual experiment for each characteristic used 60 datasets. A feature scaling method called Min-Max Normalization was applied to the input data as data preprocessing to improve the accuracy and provide faster convergence.

$$VC = M_{1 \times 14} [L_s^3 \quad L_b^3 \quad t_e^3 \quad L_s^2 \quad L_b^2 \quad t_e^2 \quad L_s \quad L_b \quad t_e \quad L_s L_b \quad L_b t_e \quad L_s t_e \quad L_s L_b t_e \quad 1]^T \quad (6)$$

In the field of machine learning, the coefficient of determination (r^2), root-mean-square error (RMSE), and mean absolute error (MAE), are mainly used to evaluate the machine learning model's performance for a regression problem. The testing results are listed in Table 12, and Figure 12 shows the scatter plots of the predicted values and the ground-truth where the r^2 scores are 0.96, 0.98 and 0.93 for the duration, color difference and visibility, respectively. Consequently, the third-order polynomial regression model can predict the duration, color difference and visibility with high R-squared, low RMSE and MAE values, which indicates a good fit.

Table 12. Evaluation metrics for the machine learning model.

| Metrics | Duration | Color Difference | Visibility |
|---------|----------|------------------|------------|
| RMSE | 3.20 | 0.22 | 0.45 |
| MAE | 2.66 | 0.18 | 0.37 |
| r^2 | 0.96 | 0.98 | 0.93 |

**Figure 12.** Scatter plots of the predictions.

5. Conclusions

A total of three evaluation aspects inclusive of the duration, color difference and visibility were investigated to understand the characteristics of high luminance LED under a dark environment. The results clearly showed that the exposure time, luminance level and background luminance were the factors that significantly influenced the afterimage characteristics. With brighter background settings, the duration and color difference can be reduced and the visibility will be effectively improved. A similar mechanism was discovered in glare measurement, which was associated with bright contrast. For this reason, a luminance-compensated mask was considered to reduce the contrast ratio of the scene for a lighting application. The consequent luminance-based compensation revealed will be discussed next by implementing an experiment for verification in future work. To better comprehend the course of afterimage converting, the duration of positive and negative afterimages requires further experiments for validation. More specific points in time are also required to establish and quantify the afterimage characteristics as functions of time.

According to the results of the regression analysis, it is suggested that the visual afterimage characteristics, duration, color difference and visibility, can be formulated by the integral of the exposure time and the luminance contrast between the test stimulus and background. The characteristics were strongly related to the exposure time multiplied by luminance contrast and showed high correlation coefficient values, whereas there was a weak correlation for the color difference under a white background. In addition, a machine learning approach, which is the third-order polynomial regression, was applied to model

the relationship between the factors and the visual perception and performed a good fit by high R-squared, low RMSE and MAE values. The model can be further used to precisely evaluate the visual characteristics as a reference for related applications.

Author Contributions: Methodology, H.-C.L.; software, H.-C.L.; formal analysis, H.-C.L.; investigation, H.-C.L.; writing—original draft preparation, H.-C.L.; writing—review and editing, P.-L.S.; supervision, P.-L.S.; project administration, P.-L.S. All authors have read and agreed to the published version of the manuscript.

Funding: This research received no external funding.

Institutional Review Board Statement: Ethical review and approval were waived for this study, due to the no requirement for the project, which was approved by the Ministry of Science and Technology in 2015.

Informed Consent Statement: Informed consent was obtained from all subjects involved in the study.

Data Availability Statement: The data presented in this study are available on request from the author.

Conflicts of Interest: The authors declare no conflict of interest.

References

1. Reidenbach, H.-D. Local susceptibility of the retina, formation and duration of afterimages in the case of Class 1 laser products, and disability glare arising from high-brightness light emitting diodes. *J. Laser Appl.* **2009**, *21*, 46–56. [[CrossRef](#)]
2. Altkorn, R.; Milkovich, S.; Rider, G. Light emitting diode safety and safety standards. In Proceedings of the IEEE Symposium on Product Safety Engineering, Schaumburg, IL, USA, 3–4 October 2005; pp. 1–5.
3. González-Pardo, A.; González-Aguilar, J.; Romero, M. Analysis of glint and glare produced by the receiver of small heliostat fields integrated in building façades. Methodology applicable to conventional central receiver systems. *Sol. Energy* **2015**, *121*, 68–77. [[CrossRef](#)]
4. Tawfeek, M.-N.; Ayoub, H.-S. Role of chromo-photometry of the vehicle interior lighting in modern automotive ergonomic. In Proceedings of the International Conference on Mathematics and Engineering Physics, Cairo, Egypt, 19–21 April 2016; Volume 8, pp. 1–11.
5. Akinsanmi, O.; Ganjang, A.-D.; Ezea, H.-U. Design and development of an automatic automobile headlight switching system. *Int. J. Eng. Appl. Sci.* **2015**, *2*, 257837.
6. Reidenbach, H.D. Prevention of Overexposure by Means of Active Protective Reactions and Magnitude of Temporary Blinding from Visible Laser Radiation. In Proceedings of the World Congress on Medical Physics and Biomedical Engineering, Munich, Germany, 7–12 September 2009; pp. 41–44. [[CrossRef](#)]
7. Ixtaina, P.; Presso, M.; Rosales, N.; Marin, G.H. Glare by Light Emitting Diode (LED) vehicle traffic signals. *Int. J. Mech. Mater. Eng.* **2015**, *10*. [[CrossRef](#)]
8. Tyukhova, Y.; Waters, C.-E. Subjective and pupil responses to discomfort glare from small, high-luminance light sources. *Light. Res. Technol.* **2019**, *51*, 592–611. [[CrossRef](#)]
9. Tyukhova, Y.; Waters, C.E. Discomfort Glare from Small, High-Luminance Light Sources When Viewed against a Dark Surround. *Leukos* **2018**, *14*, 215–230. [[CrossRef](#)]
10. Bullough, J.-D.; Boyce, P.-R.; Bierman, A.; Hunter, C.-M.; Conway, K.-M.; Nakata, A.; Figueiro, M.-G. Traffic signal luminance and visual discomfort at night. *Transp. Res. Rec.* **2001**, *1754*, 42–47. [[CrossRef](#)]
11. Collins, M. The onset of prolonged glare recovery with age. *Ophthalmic Physiol. Opt.* **1989**, *9*, 368–371. [[CrossRef](#)] [[PubMed](#)]
12. Chen, P.L.; Liao, C.H.; Li, H.C.; Jou, S.J.; Chen, H.T.; Lin, Y.H.; Tang, Y.H.; Peng, W.J.; Kuo, H.J.; Sun, P.L.; et al. A portable inspection system to estimate direct glare of various LED modules. In Proceedings of the International Conference on Optical and Photonic Engineering, Singapore, 17 July 2015; p. 95241X.
13. Sun, P.-L.; Li, H.-C.; Green, P. Evaluating CIE Unified Glare Rating of a Scene Using a Panoramic Camera. In Proceedings of the International Display Workshops, Sapporo, Japan, 3–6 December 2013; Volume 20, pp. 1143–1146.
14. Roewecklein, J.-E. *Imagery in Psychology: A Reference Guide*; Greenwood Publishing Group: Westport, CT, USA, 2004.
15. Schreuder, D.-A. Correspondence: Disturbance of vision by after-images from LED light sources. *Light. Res. Technol.* **2020**, *52*, 159–161. [[CrossRef](#)]
16. von Helmholtz, H. *Treatise on Physiological Optics*; Courier Corporation: Dover, NY, USA, 2013; Volume 3.
17. Reidenbach, H.-D. Temporary blinding from bright light sources as a significant impact on occupational safety and health. In Proceedings of the 12th International Congress of the International Radiation Protection Association (IRPA), Buenos Aires, Argentina, 19–24 October 2008.
18. Chua, F.-B.; Alvarez, T.-L.; Beck, K.-D.; Daftari, A.-P.; DeMarco, R.-M.; Bergen, M.-T.; Servatius, R.-J. Modification of saccades through light stimulation. In Proceedings of the IEEE 31st Annual Northeast Bioengineering Conference, Hoboken, NJ, USA, 2–3 April 2005; pp. 32–33.

19. Reidenbach, H.-D.; Beckmann, D.; Ghouz, I.A.; Dollinger, K. Considerations on duration of visual impairment after glare due to laser beam exposure. In Proceedings of the International Laser Safety Conference, Orlando, FL, USA, 18–21 March 2013; pp. 258–267.
20. Reidenbach, H.-D. Some quantitative aspects of temporary blinding from high brightness LEDs. In Proceedings of the Ophthalmic Technologies XVII, San Jose, CA, USA, 5 March 2007.
21. Reidenbach, H.-D. Paradigm Change for Optical Radiation–Temporary Blinding from Optical Radiation as Part of the Risk Assessment. In Proceedings of the 13th International Congress of the International Radiation Protection Association (IRPA), Glasgow, UK, 13–18 May 2012; pp. 13–18.
22. Reidenbach, H.-D. Disturbance of visual functions as a result of temporary blinding from low power lasers. In Proceedings of the Enabling Photonics Technologies for Defense, Security, and Aerospace Applications VI, Orlando, FL, USA, 16 April 2010.
23. Reidenbach, H.-D.; Ott, G.; Brose, M.; Dollinger, K. New methods in order to determine the extent of temporary blinding from laser and LED light and proposal how to allocate into blinding groups. In Proceedings of the Optical Interactions with Tissues and Cells XXI, San Francisco, CA, USA, 23 February 2010.
24. Reidenbach, H.-D. Comparison of afterimage formation and temporary visual acuity disturbance after exposure with relatively low irradiance levels of laser and led light. In Proceedings of the International Laser Safety Conference, Reno, NV, USA, 23–26 March 2009; pp. 68–77.
25. Reidenbach, H.-D. Determination of the time dependence of colored afterimages. In Proceedings of the Ophthalmic Technologies XVIII, San Jose, CA, USA, 19–20 January 2008.
26. Mikamo, M.; Slomp, M.; Raytchev, B.; Tamaki, T.; Kaneda, K. Perceptually inspired afterimage synthesis. *Comput. Graph.* **2013**, *37*, 247–255. [[CrossRef](#)]
27. Reidenbach, H.-D. Color and contrast sensitivity after glare from high-brightness LEDs. In Proceedings of the Ophthalmic Technologies XVIII, San Jose, CA, USA, 19–20 January 2008.
28. Atkinson, J. The effect of size, retinal locus, and orientation on the visibility of a single afterimage. *Percept. Psychophys.* **1972**, *12*, 213–217. [[CrossRef](#)]
29. Brémond, R.; Bodard, V.; Dumont, E.; Nouailles-Mayeur, A. Target visibility level and detection distance on a driving simulator. *Light. Res. Technol.* **2012**, *45*, 76–89. [[CrossRef](#)]
30. Vas, Z.; Bodrogi, P.; Schanda, J.; Várady, G. The non-additivity phenomenon in mesopic photometry. *Light Eng.* **2010**, *18*, 32–41.
31. Goodman, T.; Forbes, A.; Walkey, H.; Eloholma, M.; Halonen, L.; Alferdinck, J.W.A.M.; Freiding, A.; Bodrogi, P.; Varady, G.; Szalmas, A. Mesopic visual efficiency IV: A model with relevance to nighttime driving and other applications. *Light. Res. Technol.* **2007**, *39*, 365–392. [[CrossRef](#)]
32. Ito, H. Perceptual transformation of a circle and its afterimage. In *Perception ECVF Abstract*; Yumpu: Arezzo, Italy, 2007; Volume 36, p. 107.